Interannual to decadal changes in the western South Atlantic's surface circulation

Rick Lumpkin[1] and Silvia Garzoli[1]

Received 18 March 2010; revised 21 October 2010; accepted 9 November 2010; published 21 January 2011.

[1] A combination of surface drifters and altimetry is used to analyze the seasonal to interannual variability of the surface velocity field in the Brazil-Malvinas confluence of the western South Atlantic Ocean. Longer-term changes are inferred from wind and sea surface temperature fields. During the period October 1992 to December 2007, a southward shift of −0.6 to −0.9° decade^{-1} is found in the confluence latitude of the Brazil and Malvinas currents. A comparable trend is found in the latitude of the maximum wind stress curl averaged across the South Atlantic basin, allowing a proxy for the confluence latitude to be calculated for the prealtimeter time period. This longer time series suggests that the recent trend may be part of a longer-term oscillation, which has returned to values last sustained in the early 1980s. This variation does not appear to be related to the multidecadal trend in the Southern Annular Mode, but instead is inversely related to long-term variations in the sea surface temperature anomaly in the Agulhas-Benguela pathway of the eastern South Atlantic subtropical basin.

Citation: Lumpkin, R., and S. Garzoli (2011), Interannual to decadal changes in the western South Atlantic's surface circulation, *J. Geophys. Res.*, *116*, C01014, doi:10.1029/2010JC006285.

1. Introduction

[2] The South Atlantic's circulation presents several unique characteristics of significance for climate variability. This region, the main source of equatorial surface and thermocline waters [*Blanke et al.*, 1999; *Matano et al.*, 1993; *Speich et al.*, 2007], is where the circulation, and therefore its variability, impacts the climate of the surrounding continents by affecting sea surface temperature (SST) distribution through lateral advection and/or by propagating anomalies within the mixed layer [*Kushnir et al.*, 2002]. The South Atlantic is open to the Indian and Pacific Oceans, providing a gateway by which the Atlantic meridional overturning circulation communicates with the global ocean.

[3] The South Atlantic thermocline and subantarctic inflow is derived from the eastward flowing South Atlantic Current [*Stramma and England*, 1999], part of which turns northward into the Benguela Current, a broad northward flow adjacent to southwestern Africa that forms the eastern limb of the South Atlantic subtropical gyre and the origin of the upper layer water flowing northward across the equator into the North Atlantic. At 30°S, the entire current is confined between the African coast and the Walvis Ridge near the Greenwich meridian. Observations have revealed that at 30°S, the Benguela Current northward transport consists of a steady flow confined between the southern African coast and approximately 4°E, amounting to 10 Sv in the mean, and a transient flow (3 Sv in the mean) between 4°E and the Walvis Ridge [*Garzoli and Gordon*, 1996].The total westward transport in the Benguela Current Extension above 1000 m, north of the Walvis Ridge and between 18°S–33°S is estimated to be 29 Sv [*Garzoli et al.*, 1996; *Richardson and Garzoli*, 2003].

[4] The Brazil and Malvinas western boundary currents dominate the western South Atlantic circulation. The Brazil Current is one of the weakest western boundary currents in the world, with maximum poleward transport not exceeding 30 Sv, mostly confined to the upper 1000 m [*Signorini*, 1978; *Gordon and Greengrove*, 1986; *Peterson and Stramma*, 1991; *Garzoli*, 1993]. *Stommel* [1958] first suggested that this is due to what today is known as the Meridional Overturning Circulation, which requires a net northward upper ocean transport across the South Atlantic to balance the southward export of North Atlantic Deep Water. The Malvinas Current, a branch of the Circumpolar Current, flows north along the eastern boundary of the continental shelf of Argentina. At approximately 38°S, the warm salty southward flowing Brazil Current encounters the cold fresher northward flow of the Malvinas Current, generating a strong thermohaline front known as the Confluence Front (hereafter "the confluence") with lateral temperature gradients as high as 1°C per 100 m [*Gordon and Greengrove*, 1986]. After the confluence, both the Brazil and Malvinas currents turn eastward and flow offshore in a series of large-scale meanders [*Gordon and Greengrove*, 1986] and the single Brazil-Malvinas front separates into the Brazil Current Front and Subantarctic Front [*Saraceno et al.*, 2004].

[5] A marked seasonal variability in the location of the confluence, up to 900 km along the continental shelf break,

[1]Atlantic Oceanographic and Meteorological Laboratory, NOAA, Miami, Florida, USA.

has been observed from satellite observations [*Olson et al.*, 1988; *Goni and Wainer*, 2001; *Saraceno et al.*, 2004], surface observations [*Olson et al.*, 1988], and subsurface observations [*Garzoli and Bianchi*, 1987; *Garzoli and Garraffo*, 1989]. During austral summer (January, February, March) the confluence reaches its southernmost extent; during austral winter (June, July, August) it reaches its northernmost extent. Numerical studies [*Matano et al.*, 1993] indicate that this seasonal migration is governed by the curl of the wind stress, which has maximum values following a similar annual cycle. The same model also indicates that the location of the confluence depends on the mass transport of the confluent currents. However, satellite altimetry [*Vivier et al.*, 2001] suggests that Malvinas Current transport variations are not driving the annual variability of the confluence location.

[6] In addition to the seasonal variability, the latitude of separation of the Brazil Current from the coast has strong interannual variability that is forced by anomalous wind patterns south of the confluence [*Garzoli and Giulivi*, 1994]. There is no apparent correlation between wind-forced pulses in the Antarctic Circumpolar Current and the observed anomalous northward penetration of the Malvinas Current. *Witter and Gordon* [1999] concluded that interannual variations in the strength of the South Atlantic subtropical gyre, and thus of the western boundary Brazil Current, were driven by changes in the basin-wide wind stress curl, with a strong gyre in 1993–1995 and a weak gyre in 1996–1997.

[7] At longer time scales, few studies have characterized the variability of the confluence. SST observations from 1854–1994 in the well-observed region north of the mean frontal position [*Zavialov et al.*, 1999] indicate a long-term secular warming of 1.2°C–1.6°C on the continental shelf break, mostly since the 1940s, with interannual to decadal variance of up to 2.3°C^2. Using the 17°C isotherm as a marker of the confluence front, *Zavialov et al.* [1999] concluded that the northernmost (winter) confluence location exhibited significant variability at 18, 24, and ~50 years, with a generally southward drift from its northernmost location, 27.0°S in 1911, to its southernmost, 34.3°S in 1993. *Zavialov et al.* [1999] did not address what has happened to the confluence since 1993, nor address whether changes in the northernmost winter location are also representative of the mean position of the confluence front.

[8] In this study, a combination of surface drifters and altimeter data is used to analyze the seasonal to interannual variability of the surface velocity field at the confluence of the Brazil and Malvinas currents. We find that the confluence has shifted southward over the 16 year period of TOPEX/Jason satellite altimetry, with much of the shift concentrated in the first 10 years. This shift is reflected in the location of the basin-averaged wind stress curl maximum, consistent with fluctuations at the seasonal time scale, suggesting that the wind field can be used to derive a proxy for the confluence location in the prealtimeter time period. We exploit this to examine decadal fluctuations of the confluence location since 1979.

2. Data

[9] Sea level anomaly (SLA) data for this study were obtained from the 1/3° gridded Ssalto/Duacs delayed-time updated (up to four satellites) altimeter product of Archiving, Validation, and Interpretation of Satellite Oceanographic (AVISO) [*Le Traon et al.*, 1998]. This product uses data from the following altimeters for the period October 1992 to December 2007: TOPEX/Poseidon (hereafter "T/P"; start to October 2005), European Remote-Sensing Satellite (ERS) ERS-1 (start to May 1995), ERS-2 (May 1995–June 2003), Geosat Follow-On (GFO; January 2000 to December 2007), JASON-1 (April 2002 to December 2007), and Envisat (June 2003 to December 2007). SLA data are best estimated when multiple satellites are in orbit; thus, the accuracy of this product generally increases with time through the study period.

[10] Near-surface currents are derived by combining drifter velocities with wind products and altimetry. The drifters are satellite-tracked and drogued at 15 m depth [*Niiler*, 2001; *Lumpkin and Pazos*, 2007]. Ekman currents are calculated from National Centers for Environmental Prediction (NCEP) operational winds using the *Ralph and Niiler* [1999] model, with updated coefficients in the work by *Niiler* [2001]. The Ekman drift is subtracted from the total drifter velocities to derive the residual, predominantly geostrophic component of the flow. These velocities are synthesized with geostrophic velocity anomalies from the gridded altimetry, using the methodology of *Niiler et al.* [2003]. This approach uses concurrent altimetric velocity anomalies and drifter velocities to determine two spatially varying parameters: a gain coefficient, which must be multiplied with the altimeter anomalies to match the in-situ drifter eddy kinetic energy, and the time-mean unbiased current which can be added to the gain-adjusted altimetric anomalies. At every spatial point, these two parameters are calculated as a temporal average over all available drifter data. As a consequence, the methodology cannot produce temporally varying error estimates, although the densities of altimeters and drifters varies with time. However, the strength of this approach is that it combines multiple sources of information on geostrophic surface currents. This synthesis produces weekly snapshots of geostrophic near-surface currents at 1/3° resolution.

[11] In order to provide an error estimate for the location of the confluence, an alternative approach is used that relies solely upon altimetry. The AVISO SLA and their formal error estimates (also provided by AVISO) are extracted along an ascending segment of T/P ground track 163, which approximately aligns with the South American continental shelf break in the region of the Brazil-Malvinas confluence (Figure 1a). This ground track was covered by T/P from the beginning of the mission, 14 October 1992, until 15 September 2002. Jason-1 occupied this ground pass from launch in December 2001 through the latest data analyzed here (December 2007). Total sea level along this track was estimated by combining SLA with Centre National d'Etudes Spatiales–CLS09 Mean Dynamic Topography version 1.1 [*Rio et al.*, 2009]. Estimates of the confluence location from these data are not independent of estimates from the velocity product, as that uses the full gridded AVISO product which includes T/P and Jason SLA. However, as described below, the error estimate from sea height anomaly can be propagated to an error in the confluence location; thus, this approach is complementary to the approach using a synthesis of drifters, altimetry, and winds.

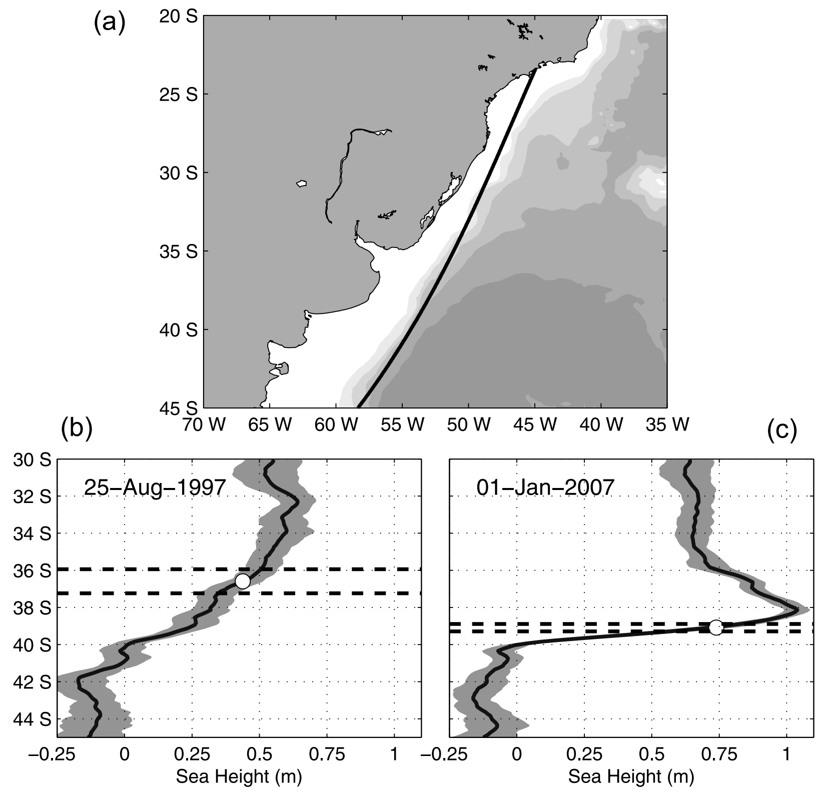

Figure 1. (a) TOPEX/POSEIDON ground track 163 superimposed on 1000 m isobaths (shading). Total sea height along ground track 163 (solid curve with shaded error bars) on (b) 25 August 1997 and (c) 1 January 2007. Circles indicates the confluence latitude, and heavy dashed curves indicate the error in confluence latitude associated with error in sea height.

[12] To analyze the behavior of the confluence for the period 1979–2007, winds, surface air pressure, and SST were obtained from the NCEP–National Center for Atmospheric Research (NCAR) version 2 Reanalysis (NNR) product [*Kalnay et al.*, 1996]. This product contains significant biases at high latitudes of the Southern Hemisphere prior to the assimilation of satellite sounder data in 1979 [*Thompson and Solomon*, 2002]; thus, we did not examine this product for earlier years for this region.

3. Mean Circulation

[13] The mean surface geostrophic circulation of the South Atlantic derived from the synthesis of surface drifter trajectories, NNR winds, and AVISO SLA are shown in Figure 2. This represents a mean for the altimeter time period 14 October 1992 through to the most recent data considered here, 31 December 2007. The mean surface characteristics of the surface circulation are well reproduced. South of Africa, the Agulhas Current enters the South Atlantic and retroflects in the mean at 22°E. The Benguela Current can be observed flowing parallel to the African coats and separating in what becomes the Benguela Current extension at around 20°S. This becomes the northern branch of the subtropical gyre and flows northwestward as the South Equatorial Current (SEC). The SEC bifurcates when it reaches the South American continent, in the mean at 16.5°S. After bifurcation, the northward north Brazil Current forms the western boundary of the elongated, clockwise equatorial gyre [*Lumpkin and Garzoli*, 2005] while the southward Brazil Current forms the western boundary of the subtropical gyre. The cold and fresh Malvinas Current is observed as a branch of the Antarctic Circumpolar Current flowing north and encountering the warm saltier Brazil Current at 38.6°S in the mean. At the confluence the flow spreads eastward in a large meander that has its southward latitude at around 45°S. It is interesting to note that the meandering and circulation in this region are very similar to that observed from Argo float data at a nominal depth of 1000 m [*Schmid and Garzoli*, 2010], indicating the strong barotropicity of the flow. Also depicted in the surface circulation and in agreement with the circulation at the intermediate water level is the presence of the Zapiola eddy [*de Miranda et al.*, 1999] at about 45°S, 45°W. East of the confluence, the Brazil and Malvinas currents flow east southeastward across the South Atlantic, with distinct cores delineating the southern edge of the subtropical gyre from the Antarctic Circumpolar Current system.

4. Variability of the Confluence

[14] The confluence latitude is defined from the merged velocity field as the latitude where the surface current vectors interpolated to the 1000 m isobath (which defines the edge of the continental shelf; Figure 1a) change direction from southward (Brazil Current) to northward (Malvinas Current) in 77 day (10 frames) low-passed velocity fields. The time series of the confluence latitude (Figure 3, top)

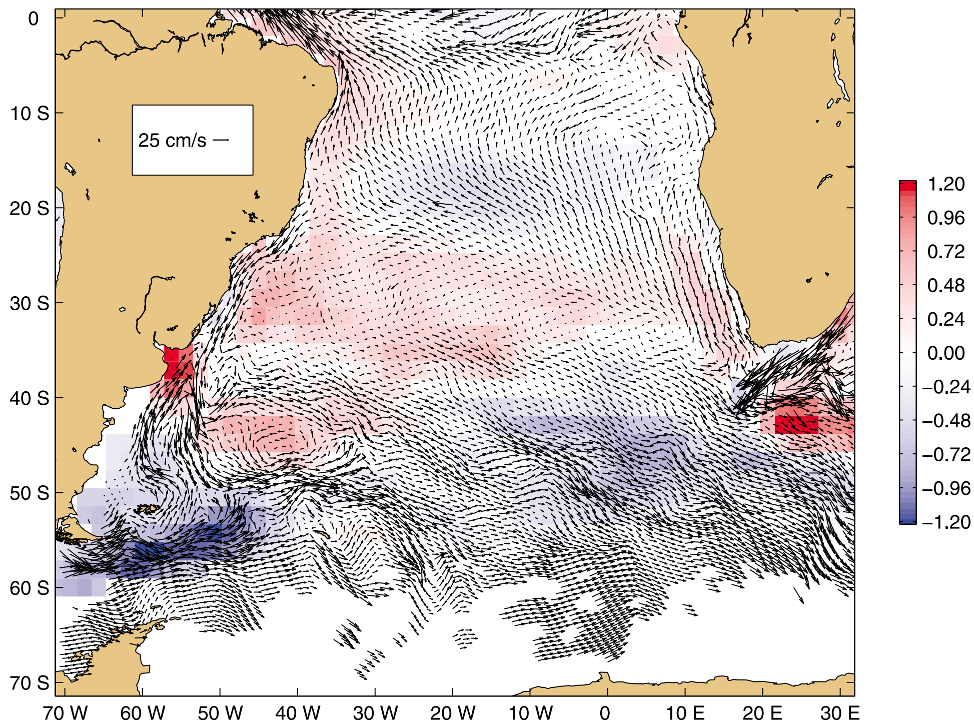

Figure 2. Mean surface geostrophic circulation of the South Atlantic derived from a synthesis of surface drifter trajectories, NCEP winds, and AVISO sea level anomalies. Color shading represents sea surface temperature anomaly trend during January 1993 to December 2002 (°C decade^{-1}) from NCEP/NCAR version 2 reanalysis [*Reynolds et al.*, 2002], with nonzero values shown only where the trend significantly exceeds zero. Warming at the Brazil-Malvinas confluence is consistent with a southward shift of the confluence front.

shows significant annual and interannual variability. A fit with an annual and semiannual cycle (superimposed on Figure 3) explains 13% of the total variance. A monthly climatology was constructed by averaging the value for every month (Figure 3, top, inset). The southernmost extension of the confluence front is observed during austral summer and the northernmost extension during winter, in agreement with previous studies [*Peterson and Stramma*, 1991; *Garzoli*, 1993; *Matano et al.*, 1993]. The maximum and minimum values of the low-passed confluence latitude for each month are also shown in Figure 3 (top, inset), showing a maximum northward extension in June 1997 and 2000 (both 35.8°S) and southward extension in March 2005 (40.3°S). This annual range is consistent with that of *Saraceno et al.* [2004], who derived the location of the front from Advanced Very High Resolution Radiometer SST data for the period 1987–1995, and showed that the front crossed the 1000 m isobath between 37°S and 38.5°S. The confluence was located north of 37°S in 1993, 1997, 1999, and 2000, but not in the subsequent 8 years.

[15] Alternatively, the confluence latitude can be defined from sea height along ascending T/P track 163 (Figure 1a), which runs from low values in the Malvinas Current to high values in the Brazil Current. The lowest and highest points are identified in sea height averaged over 77 days (as done with currents) and the confluence latitude is then identified as the latitude where sea height has climbed 3/4 of the way from the Malvinas minimum to the Brazil maximum. The arbitrary choice of 3/4 was made so that the mean location of the confluence was the same as in the velocity field definition (smaller choices produce very similar results with a mean shifted to the south). Two examples of identifying the confluence from sea height are shown in Figures 1b and 1c. The error in sea height is projected onto an error in the confluence latitude by finding the range of latitudes that meet the 3/4 criterion (dashed curves in Figures 1b and 1c). Larger error bars in the estimated confluence latitude are produced by larger errors in sea height, and also by a weak along-track sea height gradient which spreads the error over a larger latitude range. The resulting time series of confluence latitude (Figure 3, bottom) is qualitatively similar to the time series calculated from the merged velocity product, with similar peaks and troughs. Errors are largest during the northern extrema in late 1993 to early 1994, as well as in mid-1994 (which was not a dramatic peak in the velocity-derived time series), mid-1997, and mid-2000, when along-track sea height gradients are reduced.

[16] Of particular interest in the time series of confluence latitudes is the trend indicating that the confluence front has moved southward over the last 14 years, at a mean rate of $-0.86 \pm 0.19°$ decade^{-1} in the velocity-based time series (negative is southward) and $-0.64 \pm 0.20°$ decade^{-1} in the sea height (SH) based time series. A similar trend was identified in an analysis of AVISO altimetry conducted by G. Goni and P. DeNezio (unpublished data, 2005). Our standard error estimates are derived from bootstrap resam-

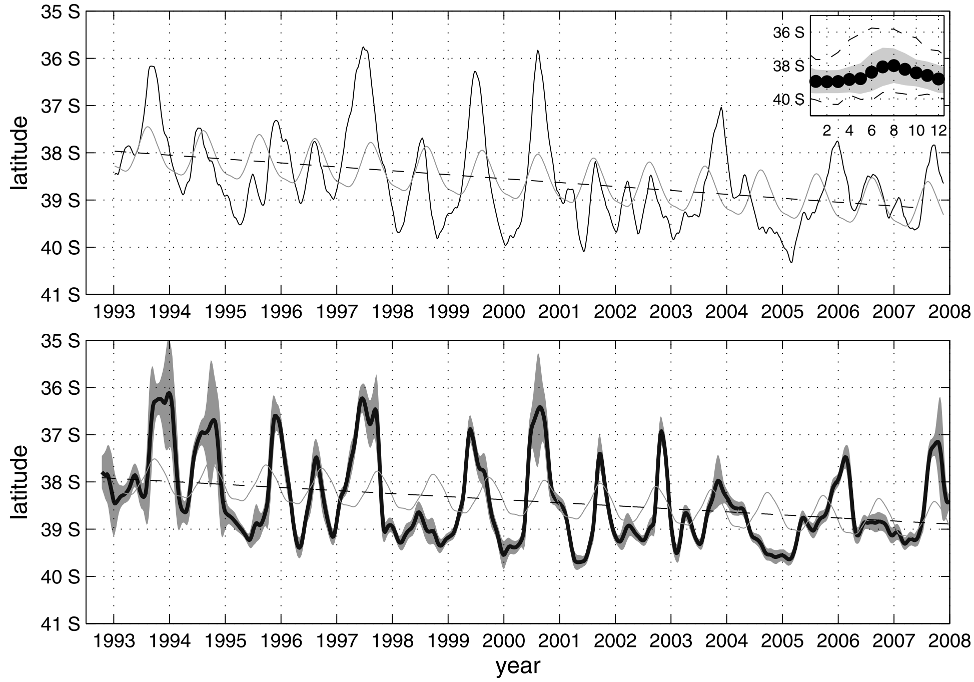

Figure 3. (top) Confluence latitude (black curve), with linear trend (dashed line), and best fit annual and semiannual (gray curve) calculated from the merged velocity field product. Inset shows the monthly climatology, with standard deviation (shading) and maximum and minimum values (dashed curves) observed in each month. (bottom) Confluence latitude determined from sea height along T/P ground track 163, with formal error estimate (shaded areas), linear trend (dashed line),and best fit annual and semiannual (shaded curve).

pling of the time series, and include the formal error in confluence latitude for the SH-based estimate. This result can be independently confirmed in the trend of NNR SST anomalies with respect to mean seasonal cycle over the same time period (Figure 2, color shading) which indicates warming of 1.64°C ± 0.25°C in the region 34°S–38°S, 53.5°W–57°W (Figure 4), centered over the continental shelf on the shallow inshore side of the southward-trending Brazil Current. Much of this southward motion took part early in the time period; the trend in the seasonal-removed confluence latitude for 1 January 1993 to 31 December 2001 was $-1.0 \pm 0.4°$ decade^{-1} (from velocity) and $-1.3 \pm 0.6°$ decade^{-1} (from SH), while the trend for 1 January 2002 to 31 December 2007 was $+0.3 \pm 0.5°$ decade^{-1} (velocity) or $+0.4 \pm 0.8°$ decade^{-1} (SH) (northward, but not significantly different from zero).

[17] The confluence location may change because of changes in the transport of the confluent currents or changes in the wind stress pattern [*Matano et al.*, 1993; *Wainer et al.*, 2000]. To investigate these possible sources of variability, an analysis is performed both of the surface transports derived from the surface current fields and of the wind field in the area. Upper ocean surface transports can be estimated by assuming that the total surface velocity is uniform in the upper 30 m and integrating the velocity across the currents. Results (Figure 5) indicate that at 32°S the surface transport is ~2 Sv to the southwest, consistent with the direction of the southward flowing Brazil Current. The direction of the transport starts to change at the confluence (38.6°S) and becomes northeastward after that (~2 Sv at 45°S), indicating the presence of the Malvinas Current. The long-term trend observed in the location of the confluence is not apparent in the surface transport values away from the confluence, suggesting that transport changes did not drive the 1993–2007 trend, although we must note that our analysis cannot detect subsurface changes not seen in the surface currents. This may be particularly important for the more stratified, baroclinic Brazil Current, which may have significant subsurface transport variability. In addition, these results do not reflect the implicit errors in our velocity product.

[18] The relation between the trend in the confluence latitude and the wind stress curl can be examined using fields from the NNR product. The SST anomalies (SSTA) were calculated by removing the mean seasonal cycle at each grid point. The spatial distribution of the SSTA trend during 1993–2002 (Figure 2, color shading) reveals that warming occurred across the basin, between 24°S–40°S. In contrast, during the same period, cooling occurred in the eastern basin between 38°S–60°S. This distribution of SSTA would produce anomalous atmospheric subsidence at ~50°S and convection at ~30°S, with consequent surface flow in geostrophic balance creating anomalous easterly winds centered on ~40°S. Such a pattern, superimposed on the background time-mean zonal wind stress (maximum Westerlies at 50°S; maximum gradient near 40°S; zero at 30°S), would shift the latitude of the maximum curl to the south as it reduces the strength of the northern edge of the Westerlies. The trend in zonal wind stress (Figure 6a) during

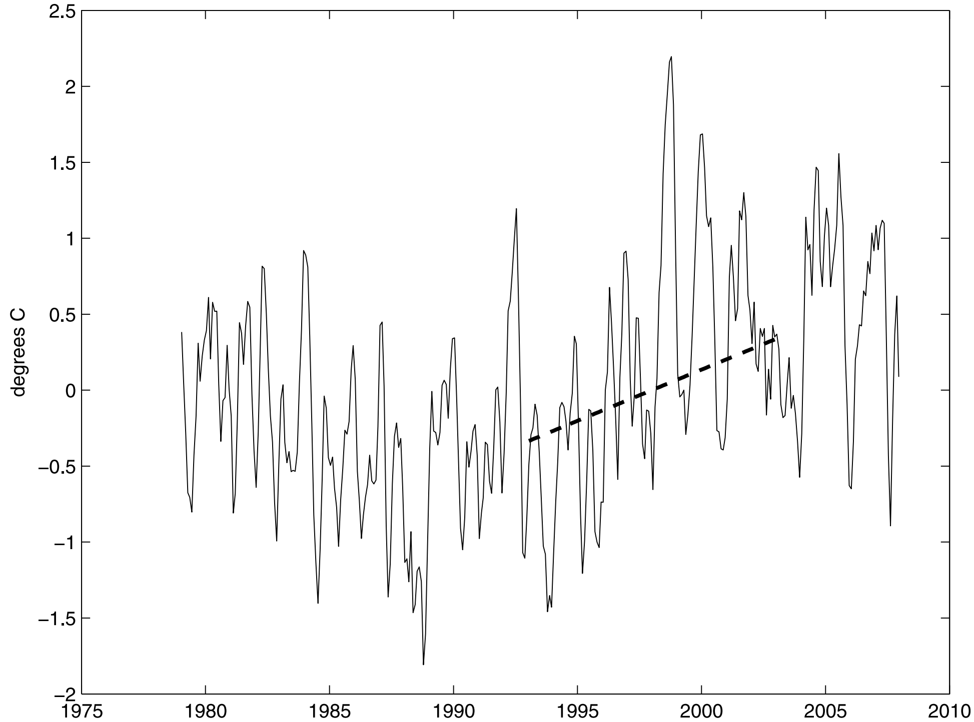

Figure 4. NCEP/NCAR version 2 reanalysis SST anomaly (°C) with respect to time-mean seasonal cycle in the region 34°S–38°S, 53.5°W–57°W. Dashed curve indicates the best fit trend during the period 1993–2002.

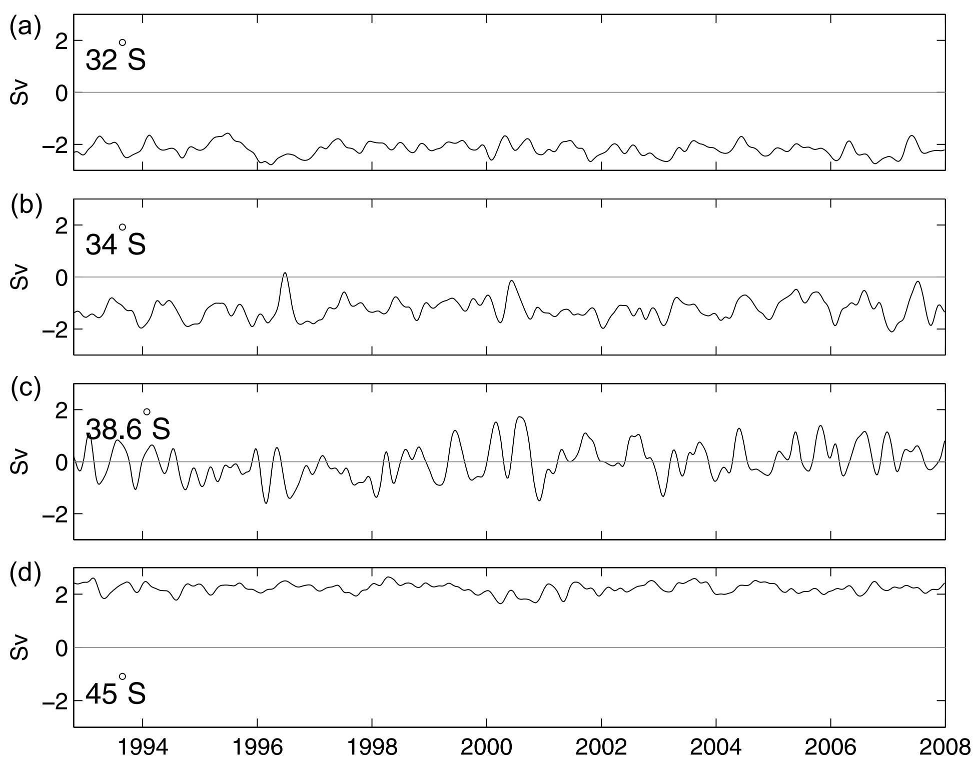

Figure 5. Upper 30 m transport (positive northward) time series of the Brazil Current at (a) 32°S, (b) 34°S at the mean location of the confluence, (c) 38.6°S, and (d) in the Malvinas Current at 45°S, calculated from near-surface currents.

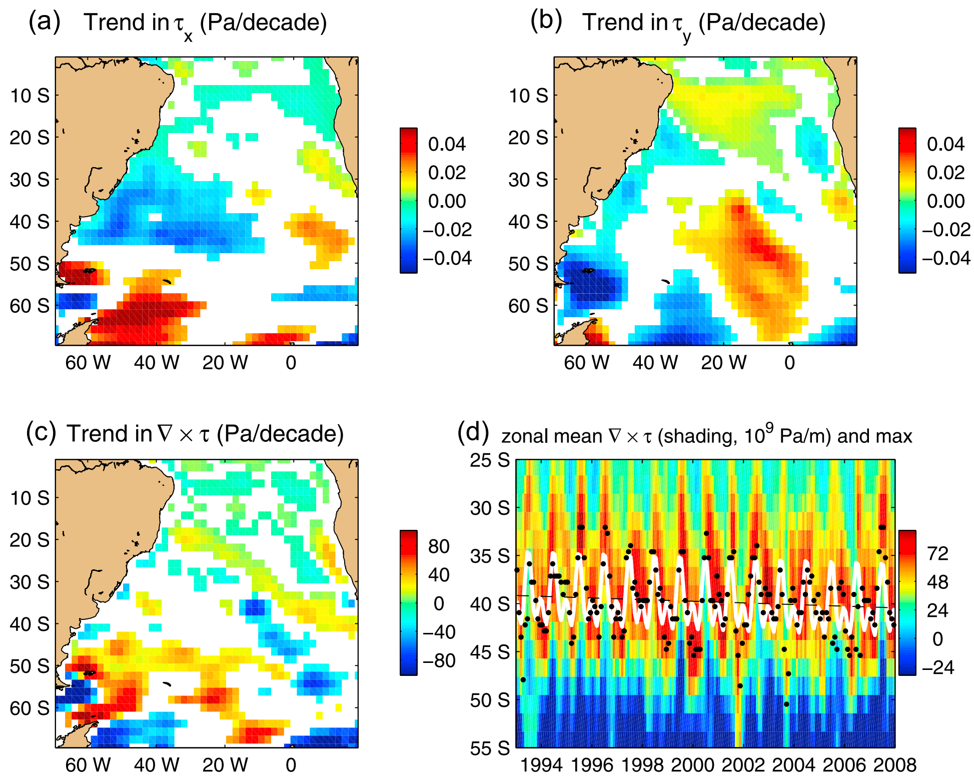

Figure 6. Trend in the (a and b) zonal and meridional components of the wind stress and (c) of the curl of the wind stress in the decade 1993–2002. Trends are not shown where they are not significantly different from zero. (d) The time series of the maximum of the curl of the wind stress across the basin as a function of time is also shown. White solid curve is the annual and semiannual fit, black dots are the maxima and the straight dashed curve indicates the slope.

1993–2008 has negative (easterly) values in the region 30°S–45°S, west of about 10°W, indicating weakening of the northern Westerlies and consistent with a southward shift in the maximum wind stress curl. The overall positive trend in zonal wind stress south of 50°S is in agreement with the trend in the Southern Annular Mode, which increased over the time period 1968–2000 [*Limpasuvan and Hartmann*, 1999; *Marshall*, 2003]. In this region, wind energy input, calculated as a scalar product of the wind stress, increased by over 12% in the past 25 years [*Huang et al.*, 2006]. Trends in the meridional wind stress (Figure 6b) are weak north of 50°S. As a consequence of these wind stress trends, the wind stress curl (Figure 6c) increased across most of the basin at the mean latitude of the confluence, and the basin-averaged maximum in the wind stress curl field (Figure 6d) shifted southward.

[19] The latitude of the maximum in the basin-averaged wind stress curl (Figure 6d) follows an annual cycle that, as previously noted by models and observations, is similar to the one followed by the confluence [*Garzoli and Giulivi*, 1994]; shifted to the north in austral winter and to the south in austral summer. A linear fit to the latitude of maximum basin-averaged stress for the period October 1992 to December 2007 has a trend of $-1.06 \pm 0.56°$ decade^{-1}, similar to the trend observed for the confluence front, suggesting that a southward shift in the maximum of the wind stress curl forced the observed trend in the confluence latitude via Sverdrup dynamics; that is, a western boundary response to the latitude of maximum equatorward interior flow [*Wainer et al.*, 2000]. If the latitude of the maximum curl is a reliable proxy for the confluence latitude, its earlier history (Figure 7, top) suggests that the 1993–2007 trend may be part of a longer-term decadal to multidecadal oscillation, which was at an unusually northward location in late 1992 through 1993 when the TOPEX/Poseidon altimeter was launched and the AVISO product began.

5. Discussion and Summary

[20] At seasonal time scales, the migration of the confluence front is driven by variations in the wind stress curl field [*Matano et al.*, 1993; *Vivier et al.*, 2001], which in turn are driven by the seasonal cycle of the South Atlantic subtropical basin SST. This can be illustrated by the correlation between the annually high-passed (to remove interannual to decadal fluctuations) latitude of basin-averaged curl and other surface properties (Figures 8a–8d). Superimposed on these seasonal variations, over the 14 years covered by the combined drifter-altimeter observations, the confluence has moved southward at a mean rate of $-0.86 \pm 0.19°$ decade^{-1} estimated from surface currents, or $-0.64 \pm 0.20°$ decade^{-1} estimated from sea height along a T/P ground track.

[21] Upper 30 m transports of the associated Brazil, Malvinas, and north Brazil currents all undergo significant seasonal and interannual variability, but no longer-term

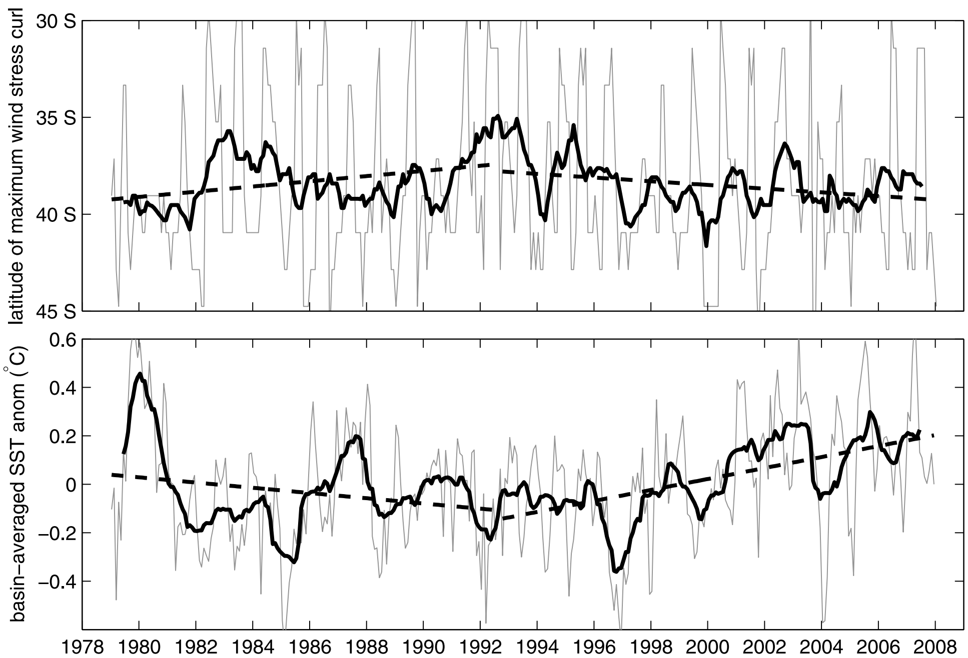

Figure 7. (top) Time series of the latitude of maximum wind stress curl averaged over the South Atlantic basin, 1979 to present, from NCEP/NCAR version 2 reanalysis. The thin gray curve indicates monthly values; the black curve is a 365 day low pass. (bottom) Time series of SST anomaly in the South Atlantic basin, calculated from NCEP/NCAR version 2 reanalysis by removing the monthly climatological mean signal at each grid point, then averaging across the basin in the latitude band 20°S–40°S.

trends were observed except in the immediate vicinity of the confluence itself.

[22] The time series of the maximum basin-averaged wind stress has a similar trend as the latitude of the confluence, $-1.06 \pm 0.56°$ decade^{-1}, with most of the southward shift happening early in the period, as seen with the confluence latitude. This strongly suggests that the trend in the confluence location is driven by the shift in the maximum of the wind stress curl at these longer time scales, as it is at the seasonal time scale. Because the curl can be calculated at earlier times than the drifter-altimetry-derived time series, the latitude of the maximum wind stress curl can serve as a proxy for the confluence latitude before October 1992. The earlier part of this proxy record (Figure 7, top) shows a weak northward trend in the location of the maximum of the curl from 1979 to 1992, suggesting that the observed trend may be part of a decadal to multidecadal oscillation that has been inferred from the northernmost winter location of the confluence front in SST records [*Zavialov et al.*, 1999]. The correlation between the low-passed (seasonal removed) latitude of maximum basin-averaged curl and various surface properties (Figures 8e–8h) suggests a similar mechanism to that acting at seasonal time scales: SST variations modifying the wind field, which shifts the confluence latitude via Sverdrup dynamics. However, while seasonal fluctuations of the confluence location are inversely correlated with SST anomalies over the entire subtropical basin, the low frequency variations are inversely correlated with SST anomalies along the Agulhas/Benguela pathway linking the Indian and Atlantic basins. (Correlations along the front in the southwest Atlantic are associated with the SST gradient across the confluence front, and are an independent confirmation of the wind stress curl proxy for confluence location.)

[23] It is clear that the confluence is not responding to the generally increasing (in the period 1968–2000) Southern Annular Mode [*Limpasuvan and Hartmann*, 1999; *Marshall*, 2003]. The SSTA in the eastern South Atlantic basin (Figure 7, bottom) has similar low frequency behavior as the wind stress curl maximum (Figure 7, top) during the period of the observations, with an opposite sign. In both cases a pronounced extreme is seen in 1992–1993.

[24] The correlation between the confluence location and SST fluctuations (Figures 8e–8h) suggests that forcing from the Indian Ocean, via an Agulhas leakage, may play a significant role in governing low frequency variations of the confluence location. However, it is interesting, albeit speculative, to note that a local positive feedback could also play a role. As described earlier, warm SST anomalies at the latitude of the confluence will alter the wind pattern such that the maximum curl shifts to the south, driving the confluence front southward. But this in turn could reinforce the SST anomaly field, as subtropical waters penetrate further south. This feedback could continue until the maximum in the wind stress curl reaches 38°S–40°S. South of that point, the superposition of an easterly anomaly on the mean westerly winds would not alter the latitude of the maximum basin-averaged curl, instead only serving to weaken the Westerlies. It is impossible to separate cause from effect in our correlation map (Figure 8h), and the simplest hypothesis to explain the band of high negative correlation in low-passed SSTA is that it reflects the meridional shifting of the

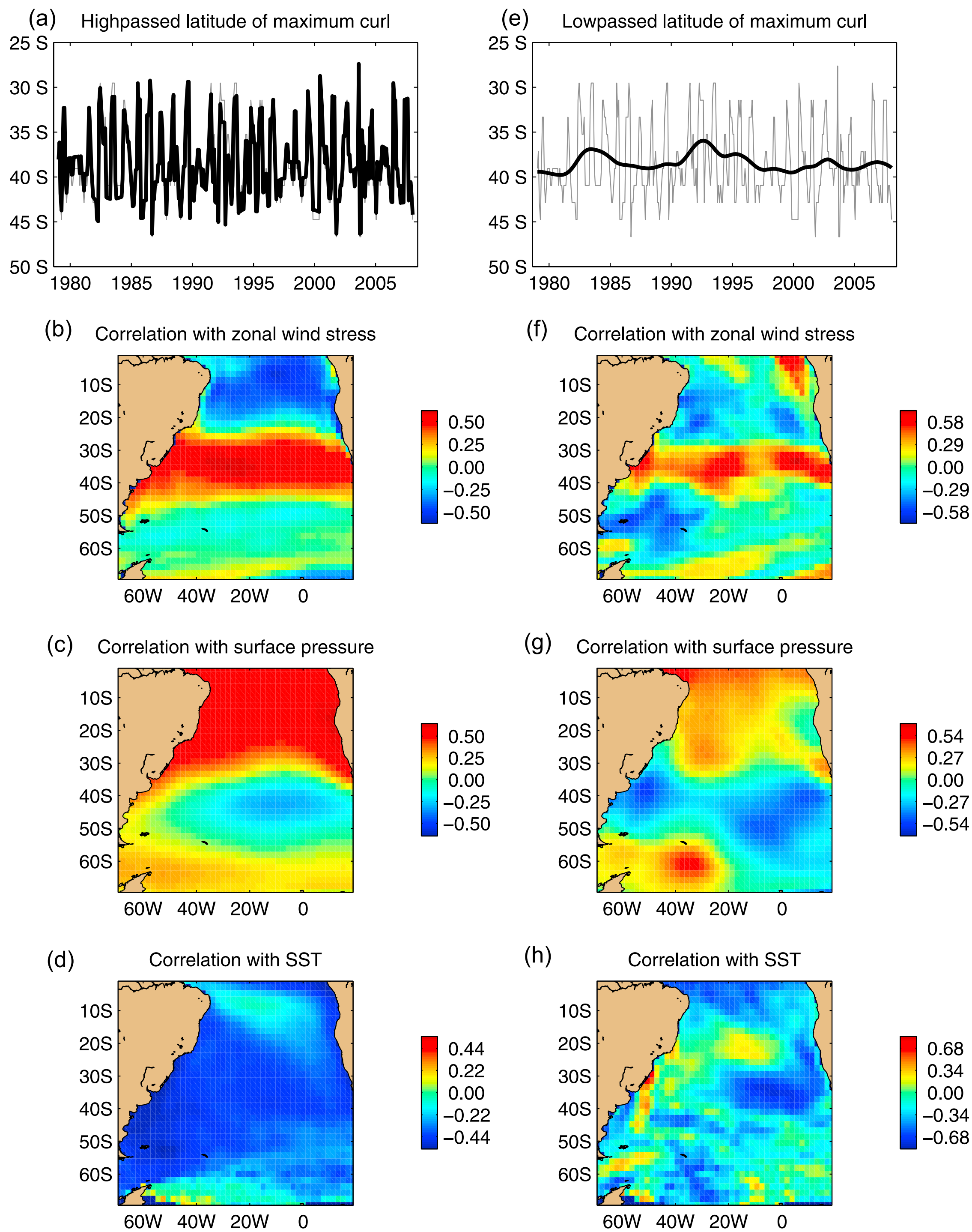

Figure 8. Latitude of the basin-averaged maximum wind stress curl, (a) high passed and (e) low passed at 365 days. The zero lag correlation coefficients between this signal and the (b) high-passed zonal wind stress, (c) surface air pressure, and (d) SST and the (f) low-passed zonal wind stress, (g) surface air pressure, and (h) SST are also shown.

front. However, such a speculative feedback mechanism cannot be ruled out, and could be tested more rigorously in the framework of a coupled ocean-atmosphere model.

[25] **Acknowledgments.** The authors were supported by NOAA's Office of Climate Observations and the Atlantic Oceanographic and Meteorological Laboratory. Conversations and input from Martin Visbeck, Gustavo Goni, Ricardo Matano, Edmo Campos, and Peter Zavialov were extremely valuable, as were two anonymous reviews. Carmen Alex performed data reduction and supporting computations. Satellite-tracked drifting buoys of the Global Drifter Program are funded as part of NOAA's Global Ocean Observing System.

References

Blanke, B., M. Arhan, G. Modec, and S. Rocheet (1999), Warm water paths in the equatorial Atlantic as diagnosed with a general circulation model, *J. Phys. Oceanogr.*, *29*, 2453–2768.

de Miranda, A. P., B. Barnier, and W. K. Dewar (1999), On the dynamics of the Zapiola Anticyclone, *J. Geophys. Res.*, *104*, 21,137–21,149, doi:10.1029/1999JC900042.

Garzoli, S. L. (1993), Geostrophic velocity and transport variability in the Brazil-Malvinas confluence, *Deep Sea Res. Part I*, *40*, 1379–1403.

Garzoli, S. L., and A. Bianchi (1987), Time-space variability of the local dynamics of the Malvinas-Brazil confluence as revealed by inverted echo sounders, *J. Geophys. Res.*, *92*, 1914–1922, doi:10.1029/JC092iC02p01914.

Garzoli, S. L., and Z. Garraffo (1989), Transports, frontal motions and eddies at the Brazil-Malvinas currents confluence, *Deep Sea Res. Part A*, *36*, 681–703.

Garzoli, S. L., and C. Giulivi (1994), What forces the variability of the south western Atlantic boundary currents?, *Deep Sea Res. Part I*, *41*, 1527–1550.

Garzoli, S. L., and A. L. Gordon (1996), Origins and variability of the Benguela Current, *J. Geophys. Res.*, *101*, 897–906.

Garzoli, S. L., A. Gordon, V. Kamenkovich, D. Pillsbury, and C. Duncombe-Rae (1996), Variability and sources of the south eastern Atlantic circulation, *J. Mar. Res.*, *54*, 1039–1071.

Goni, G., and I. Wainer (2001), Investigation of the Brazil Current front dynamics from altimeter data, *J. Geophys. Res.*, *106*, 31,117–31,128, doi:10.1029/2000JC000396.

Gordon, A. L., and C. L. Greengrove (1986), Geostrophic circulation of the Brazil-Falkland confluence, *Deep Sea Res. Part A*, *33*, 573–585.

Huang, R. X., W. Wang, and L. L. Liu (2006), Decadal variability of wind energy input to the world ocean, *Deep Sea Res. Part II*, *53*, 31–41.

Kalnay, E., et al. (1996), The NCEP/NCAR 40-year reanalysis project, *Bull. Am. Meteorol. Soc.*, *77*, 347–471.

Kushnir, Y., W. A. Robinson, I. Bladé, N. M. J. Hall, S. Peng, and R. Sutton (2002), Atmospheric GCM response to extratropical SST anomalies: Synthesis and evaluation, *J. Clim.*, *15*, 2233–2256.

Le Traon, P., F. Nadal, and N. Ducet (1998), An improved mapping method of multisatellite altimeter data, *J. Atmos. Oceanic Technol.*, *15*, 522–534.

Limpasuvan, V., and D. L. Hartmann (1999), Eddies and the annular modes of climate variability, *Geophys. Res. Lett.*, *26*, 3133–3136, doi:10.1029/1999GL010478.

Lumpkin, R., and S. L. Garzoli (2005), Near-surface circulation in the tropical Atlantic Ocean, *Deep Sea Res. Part I*, *52*, 495–518, doi:10.1016/j.dsr.2004.09.001.

Lumpkin, R., and M. Pazos (2007), Measuring surface currents with Surface Velocity Program drifters: The instrument, its data, and some recent results, in *Lagrangian Analysis and Prediction of Coastal and Ocean Dynamics*, edited by A. Griffa et al., chap. 2, pp. 39–67, Cambridge Univ. Press, Cambridge, U. K.

Marshall, G. J. (2003), Trends in the Southern Annular Mode from observations and reanalyses, *J. Clim.*, *16*, 4134–4143.

Matano, R. P., M. G. Schlax, and D. B. Chelton (1993), Seasonal variability in the South Atlantic, *J. Geophys. Res.*, *98*, 18,027–18,035.

Niiler, P. P. (2001), The world ocean surface circulation, in *Ocean Circulation and Climate*, *Int. Geophys. Ser.*, vol. 77, edited by G. Siedler, J. Church, and J. Gould, pp. 193–204, Academic, New York.

Niiler, P. P., N. A. Maximenko, G. G. Panteleev, T. Yamagata, and D. B. Olson (2003), Near-surface dynamical structure of the Kuroshio Extension, *J. Geophys. Res.*, *108*(C6), 3193, doi:10.1029/2002JC001461.

Olson, D., G. P. Podesta, R. H. Evans, and O. B. Brown (1988), Temporal variations in the separation of Brazil and Malvinas currents, *Deep Sea Res. Part A*, *35*, 1971–1990.

Peterson, R. G., and L. Stramma (1991), Upper-level circulation in the South Atlantic Ocean, *Prog. Oceanogr.*, *26*, 1–73.

Ralph, E. A., and P. P. Niiler (1999), Wind-driven currents in the tropical Pacific, *J. Phys. Oceanogr.*, *29*, 2121–2129.

Reynolds, R. W., N. A. Rayner, T. M. Smith, D. C. Stokes, and W. Wang (2002), An improved in situ and satellite SST analysis for climate, *J. Clim.*, *15*, 1609–1625.

Richardson, P. L., and S. L. Garzoli (2003), Characteristics of intermediate water flow in the Benguela Current as measured with RAFOS floats, *Deep Sea Res. Part II*, *50*, 87–118.

Rio, M.-H., P. Schaeffer, G. Moreaux, J.-M. Lemoine, and E. Bronner (2009), A new mean dynamic topography computed over the global ocean from GRACE data, altimetry, and in-situ measurements, paper presented at OceanObs'09, Eur. Space Agency, Venice, Italy, 21–25 Sept.

Saraceno, M., C. Provost, A. Piola, J. Bava, and A. Gagliardini (2004), Brazil Malvinas frontal system as seen from 9 years of advanced very high resolution radiometer data, *J. Geophys. Res.*, *109*, C05027, doi:10.1029/2003JC002127.

Schmid, C., and S. L. Garzoli (2010), New observations of the spreading and variability of the Antarctic Intermediate Water in the Atlantic, *J. Mar. Res.*, *67*, 815–843.

Signorini, S. R. (1978), On the circulation and the volume transport of the Brazil Current between the Cape of São Tomé and Guanabara Bay, *Deep Sea Res.*, *25*, 481–490, doi:10.1016/0146-6291(78)90556-8.

Speich, S., B. Blanke, and W. Cai (2007), Atlantic meridional overturning and the Southern Hemisphere supergyre, *Geophys. Res. Lett.*, *34*, L23614, doi:10.1029/2007GL031583.

Stommel, H. M. (1958), *The Gulf Stream: A Physical and Dynamical Description*, 202 pp., Univ. of Calif. Press, Berkeley, Calif.

Stramma, L., and M. England (1999), On the water masses and mean circulation of the South Atlantic Ocean, *J. Geophys. Res.*, *104*, 20,863–20,883, doi:10.1029/1999JC900139.

Thompson, D. W. J., and S. Solomon (2002), Interpretation of recent Southern Hemisphere climate change, *Science*, *296*, 895–899, doi:10.1126/science.1069270.

Vivier, F., C. Provost, and M. P. Meredith (2001), Remote and local forcing in the Brazil-Malvinas region, *J. Phys. Oceanogr.*, *31*, 892–913.

Wainer, I., P. Gent, and G. Goni (2000), Annual cycle of the Brazil-Malvinas Confluence region in the National Center for Atmospheric Research climate system model, *J. Geophys. Res.*, *105*, 26,167–26,177, doi:10.1029/1999JC000134.

Witter, D., and A. Gordon (1999), Interannual variability of South Atlantic circulation from 4 years of TOPEX/POSEIDON satellite altimeter observations, *J. Geophys. Res.*, *104*, 20,927–20,948, doi:10.1029/1999JC900023.

Zavialov, P. O., I. Wainer, and J. M. Absy (1999), Sea surface temperature variability off southern Brazil and Uruguay as revealed from historical data since 1854, *J. Geophys. Res.*, *104*, 21,021–21,032, doi:10.1029/1998JC900096.

S. Garzoli and R. Lumpkin, Atlantic Oceanographic and Meteorological Laboratory, NOAA, 4301 Rickenbacker Cswy., Miami, FL 33149, USA. (rick.lumpkin@noaa.gov)